SPECTROPHOTOMETRY OF SUPERNOVAE

R. P. KIRSHNER

Hale Observatories, California Institute of Technology, Carnegie Institution of Washington,
Pasadena, Cal., U.S.A.

Abstract. Absolute spectral energy distributions for supernovae of both types I and II have been obtained. These observations demonstrate three facets of supernova spectra. First, both SN I's and SN II's have a continuum that varies slowly and uniformly with time, and which carries the bulk of the radiated flux at early epochs. Second, some lines in both SN I's and SN II's have P Cygni profiles: broad emissions flanked on their violet edges by broad absorptions. Third, some lines are common to SN I's and SN II's and persist throughout the evolution of the spectrum. The continuum temperatures for both SN I's and SN II's are about 10000 K at the earliest times of observation and drop in one month's time to about 6000 K for SN II's and about 7000 K for SN I's. After several months, the continuum may cease to carry the bulk of the flux, which might be in emission lines, but continues to exist, as shown by the presence of absorption lines. The P Cygni line profiles indicate expansion velocities of 15000 km s^{-1} in SN II's and 20000 km s^{-1} in the SN I 1972e in NGC 5253. Line identifications for SN II's include Hα, Hβ, H and K of Ca II, the Ca II infrared triplet at λ8600, the Na I D-lines, the Mg I b-lines at λ5174, and perhaps Fe II. The [O I] lines $\lambda\lambda$6300, 6363 and [Ca II] lines $\lambda\lambda$7291, 7323 appear after eight months. For SN I's, the lines identified are H and K of Ca II, the infrared Ca II lines, the Na I D-lines, and the Mg I b-lines. There is some evidence that Balmer lines are present two weeks after maximum. The strong and puzzling λ4600 features drifts with time from λ4600 near maximum light to λ4750 after 400 days.

1. Introduction

Although supernova explosions are at the root of many modern astrophysical theories for nucleosynthesis, cosmic rays, pulsars, black holes, and the interstellar medium, the study of the actual event has not progressed rapidly since Minkowski's (1939) classic work. This valuable investigation of the SN I 1937c, recently rendered even more useful by Greenstein and Minkowski (1973), still provides the observational evidence used to analyze the supernova event empirically.

Supernovae appear at random, and are only found by time-consuming searches. Even though they may be of 13th mag. at first, within a month spectroscopic observations become quite difficult. Thus, it is no surprise that the available information has been limited.

Recently, the multichannel spectrometer (Oke, 1969) has been employed by J. B. Oke, L. Searle, M. V. Penston, J. E. Gunn, and J. L. Greenstein, to obtain series of spectral energy distributions for supernovae of both type I and type II. This instrument, attached to the 200-in. (508 cm) telescope, produces a quantitative spectrum covering the wavelength range $\lambda\lambda$3200–10000. The resolution of 20 to 160 Å is well suited to the broad indistinct features of supernovae spectra.

This work was given impetus by the appearance of several relatively bright supernovae, especially SN I 1972e. For that supernova, an extensive series of observations has been obtained, using both the 200-in. telescope with multichannel spectrometer and the Palomar 60-in. (152 cm) telescope with a single channel scanner.

Much of this work has been reported recently (Kirshner *et al.* 1973a, b). Some of the

observations reported there are illustrated in Figure 1, which shows scans for the SN II 1970g in M 101, and in Figures 3, 4, 5 of the SN I 1972e in NGC 5253. The purpose of this contribution is to give a brief summary of the principal results of these preliminary investigations.

2. Supernovae of Type II

2.1. CONTINUUM

Figure 1 exhibits spectral scans for a type II supernova. The first scan of 1970g in M 101 was made soon after its discovery, and near maximum light. Here the continuum is well defined and resembles that of a blackbody at about 9500 K, although the blackbody which fits best between $\lambda 5000$ and $\lambda 10000$ is brighter than the supernova in the ultraviolet. The scans of 1970g for JD 837, made about 1 month after discovery, resembles a blackbody in the vicinity of 6000 K. Both at the earliest epoch and at age one month, the continuum transports most of the energy.

After 250 days, observations show strong emission bands, with some evidence for a continuum. The continued presence at these late dates of absorption features which are identical with those of early times argues that the continuum, though faint, is still present.

We interpret these observations as indicating that SN II's have optically thick and cooling photospheres. Comparison of the observed flux with the expected blackbody flux at a distance of 7 Mpc for M 101 gives a photospheric radius of order 1×10^{15} cm at age one month. Study of the expansion of the photosphere may lead to a method for determining the distances to supernovae by purely astrophysical methods.

2.2. LINE SHAPES

When the continuum dominates the energy distribution, all of the strongest line features in the spectra of SN II's have P Cygni shapes. The broad emission bands are flanked on the short wavelength side by a broad absorption trough. The line profiles at $\lambda\lambda 8600, 6500, 4800, 4300$, and 3950 can all be characterized in this way, even though they are not identical.

The most clearly defined profile is at $\lambda 8600$, where the continuum is smooth. Figure 6, taken from the scan of SN 1970g on JD 837 shows that this line has nearly zero net equivalent width. One simple interpretation of this profile is that the line is formed by scattering photospheric radiation in a spherically symmetric and differentially expanding reversing layer. Then the violet shifted absorption is due to gas along our line of sight to the photosphere absorbing the radiation, and re-emitting it in another direction. Similarly, the emission comes from the re-emitted radiation from the rest of the expanding envelope. In the simplest cases, the net zero width is the natural consequence of pure scattering as from a resonance line.

The violet edge of absorption, at $v = -15000$ km s^{-1} is shifted about as much as the red edge of emission. For SN 1969l in NGC 1058, the observed shifts are also about 15000 km s^{-1}.
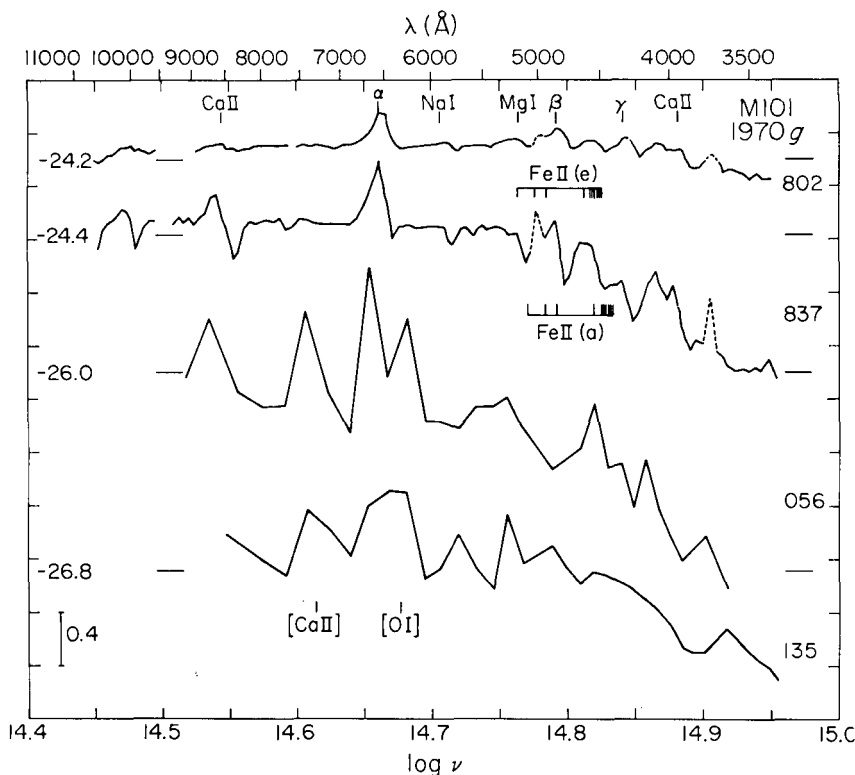
Fig. 1. Energy distributions for type II SN 1970g in NGC 5457 (M101). The horizontal scale is $\log \nu$ where ν is the observed frequency in Hz. A wavelength scale is shown at the top of the figure. The vertical scale is $\log f_\nu$ where f_ν is the observed flux in ergs s⁻¹ cm⁻² Hz⁻¹. The absolute flux level is indicated at the left of each energy distribution along with a tick mark which is repeated at the right. Each energy distribution is identified by the last three digits of the Julian Day when the observation was made. Representative standard deviation bars are shown where they are significant towards the ends of each scan. Errors in the center part of each energy distribution (i.e. $14.55 \leqslant \log \nu \leqslant 14.85$) are normally too small to be shown. The description above also applies to Figures 2–5. The dotted portions of the top two energy distributions are the emission lines $\lambda 3727$ of [O II] and $\lambda 5007$ of [O III] which come from the background H II region. For the bottom two energy distributions the background H II region [which had been observed previously (Searle, 1971)] has been subtracted as well as possible. Possible line identifications of the emission peaks are marked. The positions of the strongest expected Fe II lines are shown. The emission wavelengths are plotted without velocity corrections. The absorption wavelengths are displaced by 0.008 in $\log \nu$ to the violet corresponding to the velocity of other absorption minima. (By permission of the *Astrophysical Journal*.)

2.3. LINE IDENTIFICATIONS

2.3.1. *Balmer Lines*

As reported by many observers for many years, the Balmer series is certainly present in the spectra of SN II's, at all the epochs observed. The Hα profile, shown in Figure 6 for SN 1970g, indicates net emission, with the emission peak centered near the rest wavelength, in the rest frame of M 101. The width of this line, from the red edge of

emission to the blue edge of the absorption is about the same as for the $\lambda 8600$ line. This suggests that the two lines are formed over the same volume, so that conditions inferred from the Hα line apply to the entire reversing layer.

On JD 802, the observed net flux from SN 1970g in M 101 was about 3.6×10^{12} erg cm^{-2} s^{-1}. Using a distance of 7 Mpc, this corresponds to 2×10^{39} erg s^{-1} emitted at the source. At about 10000 K, this requires $n_e^2 V = 3.5 \times 10^{64}$ cm^{-3}. Since the reversing layer is somewhat bigger than the photosphere, we estimate a radius of 10^{15} cm, which implies an electron density $n_e \approx 3 \times 10^9$ cm^{-3}, and thus 3×10^{24} electrons cm^{-2} along the line of sight. Similarly, the net Hα emission for JD 837 combined with a velocity 1.5×10^9 cm s^{-1} and an age of about 40 days gives $n_e \simeq 3 \times 10^8$ and a column density of about 2×10^{24} cm^{-2}.

It may be significant that the column density is just adequate to make the reversing layer optically thick in electron scattering. A lower bound to the mass in the envelope comes from assuming the hydrogen is fully ionized. Then $M > 0.1\ M_\odot$.

2.3.2. *Lines of* Ca II, Na I, *and* Mg I

The continuum and Balmer lines provide information on the physical state of the expanding envelope. We deduced a differentially expanding cloud with $n_e \simeq 10^9$, irradiated by a photosphere of $T = 5000$–10000 K, diluted by a factor of $W \approx 0.01$. The lines to be anticipated are those arising from the ground state or metastable states of ions that are abundant in such an environment. In general, lines present in A and F-type supergiants and in shells surrounding A and F stars might be expected to appear.

The strongest observed features, aside from the Balmer lines are at $\lambda 3950$ and $\lambda 8600$. Consideration of the physical state of the envelope leads to the suggestion that $\lambda 3950$ is due to the H and K lines of Ca II and that the $\lambda 8600$ feature is due to the Ca II infrared triplet $\lambda\lambda 8498, 8542, 8662$. The triplet arises from the metastable $3d\ ^2D$ level, and the upper level is the upper level of the H and K transitions.

The next strongest features are $\lambda 5890$ and $\lambda 5180$. The first could be either $\lambda 5876$ of He I or $\lambda 5890$ of Na I. The sodium seems most likely, as none of the other strong triplet lines of He I is apparent. Although most of the sodium will be ionized, the residual neutral sodium can account for the observed modest line strength.

Analogously, the resonance lines of Ca I $\lambda 4226$ should be present, even though most calcium is ionized. This line falls in a blended region of the spectrum, and could be as strong as the D-lines without being detected. We also expect the Mg I b-lines arising from metastable levels to be strong at $\lambda 5174$. This probably accounts for the feature at $\lambda 5180$.

2.3.3. *The Feature at* $\lambda 4600$

The prominent feature at $\lambda 4600$ is reminiscent of the similar feature in Nova Herculis (Stratton, 1934). There, the feature is attributed to Fe II. A similar situation is very likely to arise here. Accordingly, the emission and blueshifted absorptions for the relevant Fe II lines are plotted in Figure 1. The fit is not exact but does suggest

that the feature at $\lambda 4600$ is at least partly due to Fe II. A similar conclusion, based only on the absorption features, has already been reached by Patchett and Branch (1972).

2.3.4. [O I]

In Figure 1, the scans obtained 8 months or more after maximum light show the appearance of two strong emission features at $\lambda 6300$ and $\lambda 7300$.

The feature at $\lambda 6300$ is likely to be the [O I] doublet at $\lambda 6300$ and $\lambda 6363$. Although blended with Hα in these scans, slit spectra at comparable times demonstrate the clear separation of the two lines.

The appearance of this line, and its strength relative to Hα, indicate that the envelope has both recombined and grown less dense since maximum light.

2.3.5. [Ca II]

There are two possible identifications for the strong emission line at $\lambda 7300$ which occurs in the later phases of SN II's. It could be $\lambda 7320 + \lambda 7330$ of [O II] or it could be $\lambda 7291 + \lambda 7323$ of [Ca II]. The excitation potential of the upper level of the $\lambda 7320$ transition in [O II] is 4 eV and it is unclear how this could be excited collisionally without producing at the same time other permitted and forbidden lines of the abundant once ionized metals with comparable intensities, as happens, for example, in the spectra of novae. The great strength of this line at $\lambda 7300$ in the later phases of SN II's and the fact that, in the case of SN II 1969l in NGC 1058, it is not accompanied by any other emissions that can be identified with other well-known forbidden lines, leads us to reject the identification with [O II].

The identification with $\lambda 7291$ and $\lambda 7323$, on the other hand, provides a natural explanation of the behavior of this line. The [Ca II] lines are an intersystem transition that connects the metastable lower level of the $\lambda 8600$ transitions with the ground state of the ion. In the first month after maximum light the $\lambda 8600$ line in SN II's shows a P Cygni profile with a zero net equivalent width. This implies that the depopulation of the $3d\,^2D$ level is almost exclusively by radiative reabsorptions in the $\lambda 8600$ line rather than by alternative processes, the most important of which are expected to be collisional and radiative transitions to the ground state and photo-ionizations resulting from absorption of Lα photons.

At some time between 1 and 8 months following maximum light, the energy density in the radiation field has dropped sufficiently that depopulations via the intersystem transition are more probable than radiative reabsorptions. When these reabsorptions eventually become negligible and the density has fallen to the point that radiative downward transitions from $3d\,^2D$ are more probable than collisionally induced ones, absorptions in H and K, plus collisions to the upper state, feed a cascade via $\lambda 8600$ and $\lambda 7300$. In these circumstances the lines at $\lambda 8600$ and $\lambda 7300$ would have very nearly the same intensity as observed. It will be of importance to follow in detail the development of the $\lambda 7300$ line in SN II's between 1 month and 8 months after maximum light.

3. Supernovae of Type I

3.1. CONTINUUM

As shown in Kirshner *et al.* (1973a), the overall energy distributions from 2.2 μ to 0.33 μ of the type I SN 1972e in NGC 5253 can be well represented by blackbodies. The best fit at the earliest epochs has $T = 10\,000$ K, which falls smoothly and gradually to 7000 K in 2 weeks. Further decreases in temperature were quite slow for at least 3 weeks. The smooth and gradual evolution of the spectrum demonstrates that the type I spectrum is not a superposition of emission bands: just as in type II's the bulk of the energy is radiated in a continuum. As in type II, the photospheric radius in the first month is of order 10^{15} cm.

3.2. LINE PROFILES

As Figure 2 demonstrates, the spectra of SN I's are more complicated than those of SN II's. There, scans of the two types are shown at comparable phases. It also demonstrates that the strongest and most persistent features of SN II's appear among the strongest and most persistent features in SN I's. The outstanding examples are the features near $\lambda 3950$ and $\lambda 8600$, which we identified in SN II's with Ca II: they are prominent in type I spectra during the entire interval covered by observations.

The lines in SN I's have a characteristic P Cygni profile, as shown in Figure 6.
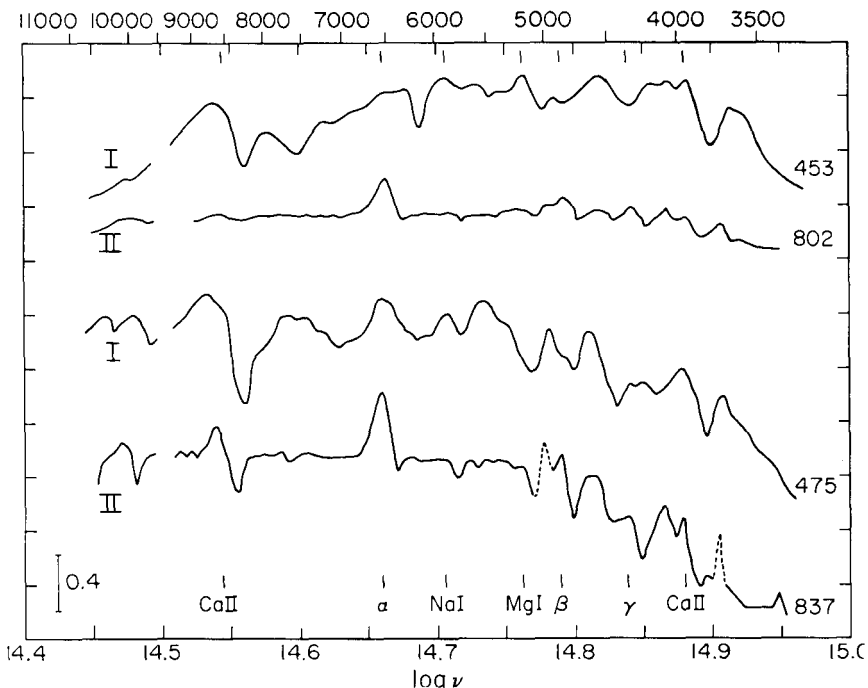

Fig. 2. Comparison of spectral energy distributions of type I and type II supernovae at two selected phases. The type I curves are from SN 1972e, while those for type II are from SN 1970g. (By permission of the *Astrophysical Journal*.)
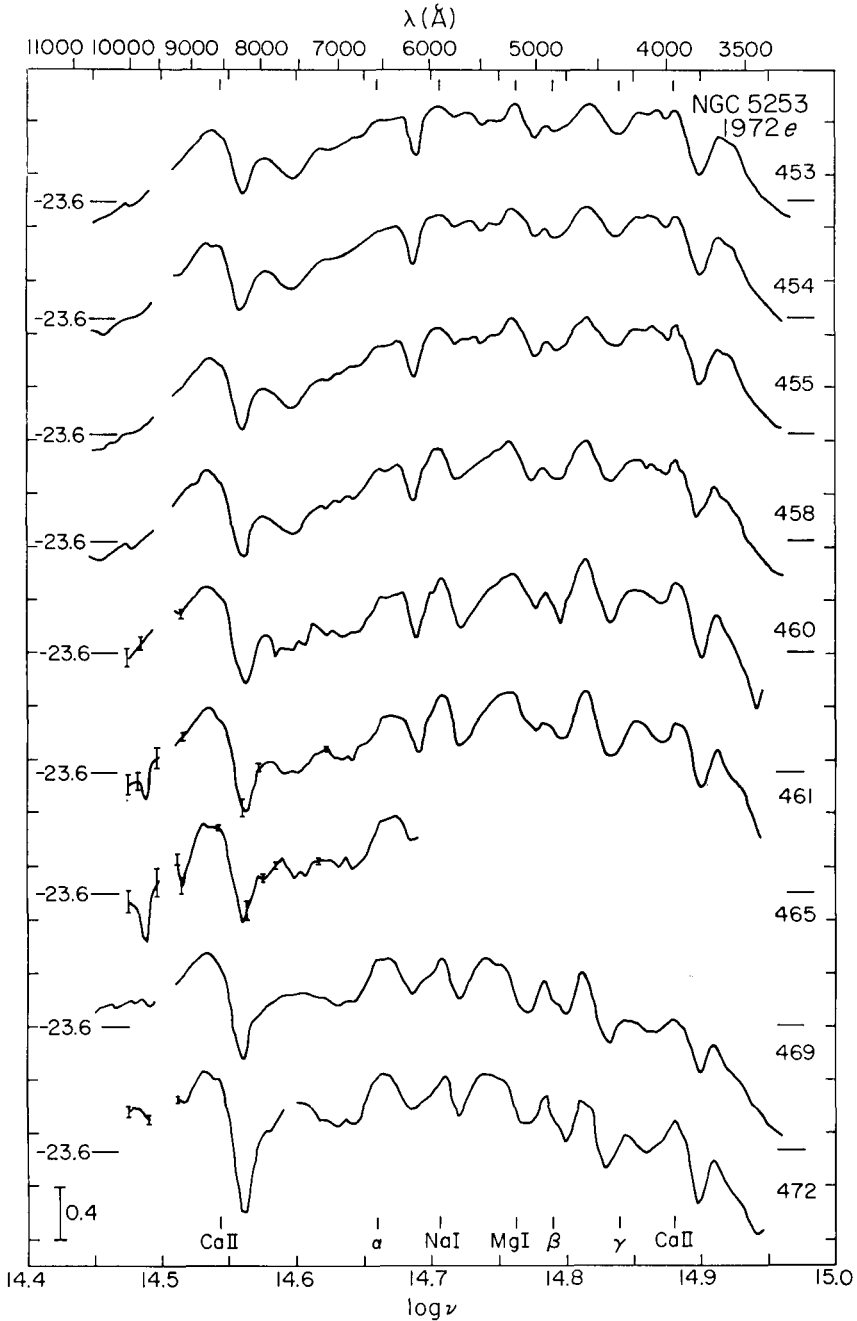
Fig. 3. Spectral energy distributions for SN 1972e in NGC 5253. Description is the same as in Figure 1. The smoothness of the distributions as drawn is real since the curves go through all measured points. Possible identifications of emission peaks are shown. The Balmer lines Hα, Hβ, and Hγ are included but do not necessarily imply the existence of these lines. (By permission of the *Astrophysical Journal*.)
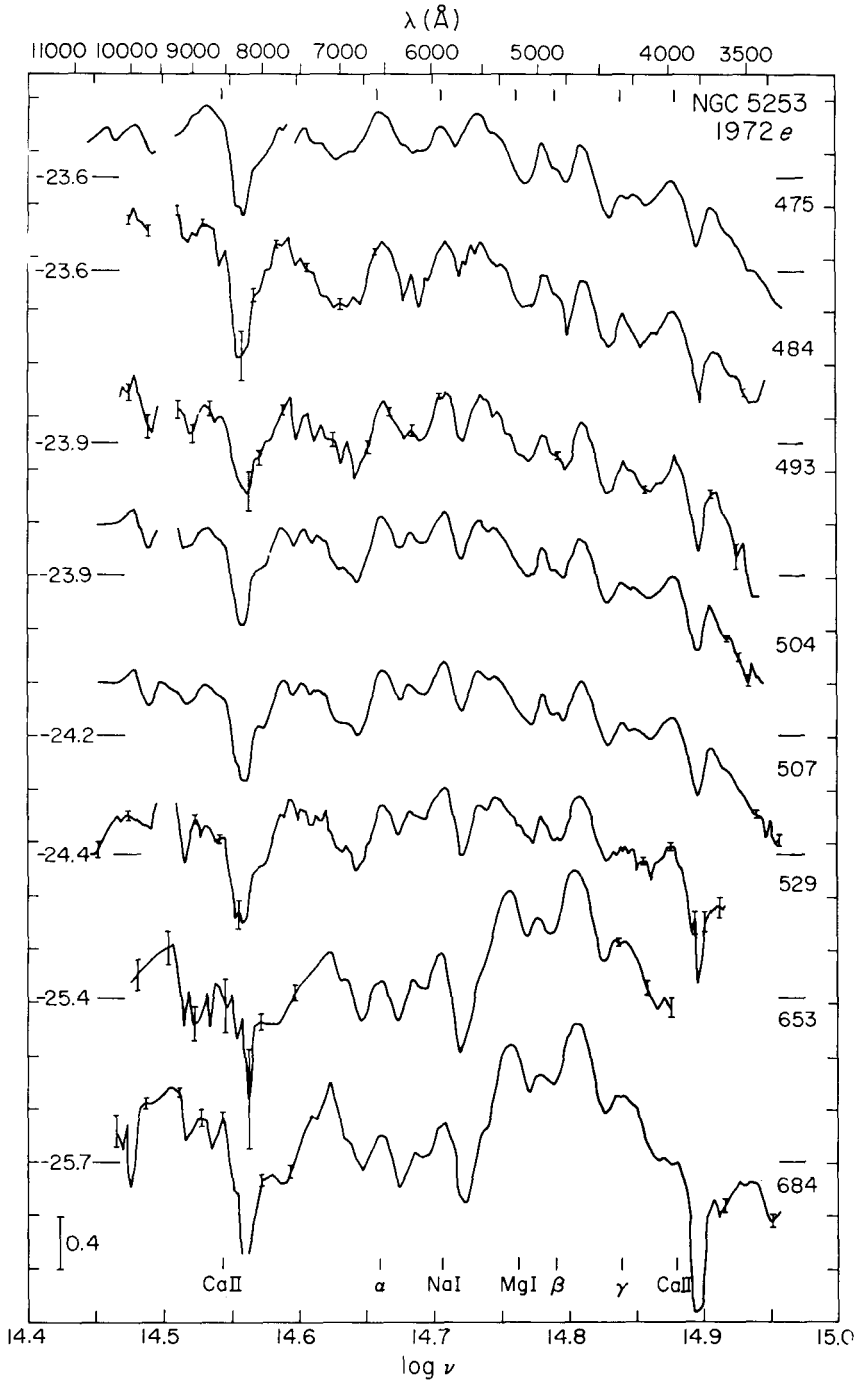
Fig. 4. Continuation of Figure 3. (By permission of the *Astrophysical Journal*.)

Here the $\lambda 8600$ line shape is somewhat irregular, but the essential feature of symmetrical emission near the rest wavelength and blueshifted absorption is present. The red edge of the emission peak indicates a recession velocity of about 20000 km s^{-1} while the blue edge of the absorption, though less well defined, shows a shift that is at least as large.

3.3. LINE IDENTIFICATIONS IN TYPE I'S

Four strong features in Figures 3 and 4 persist through the supernova's early evolution. Each consists of an emission peak and a blueshifted absorption. The emission peak wavelengths are at $\lambda 8700$, $\lambda 5890$, $\lambda 4600$, and $\lambda 3970$.

The striking fact that these four lines coincide with the strongest non-hydrogen features in the spectra of type II's leads to the conclusion that they are the *same* features and that there exists an underlying similarity to the two types of supernovae.
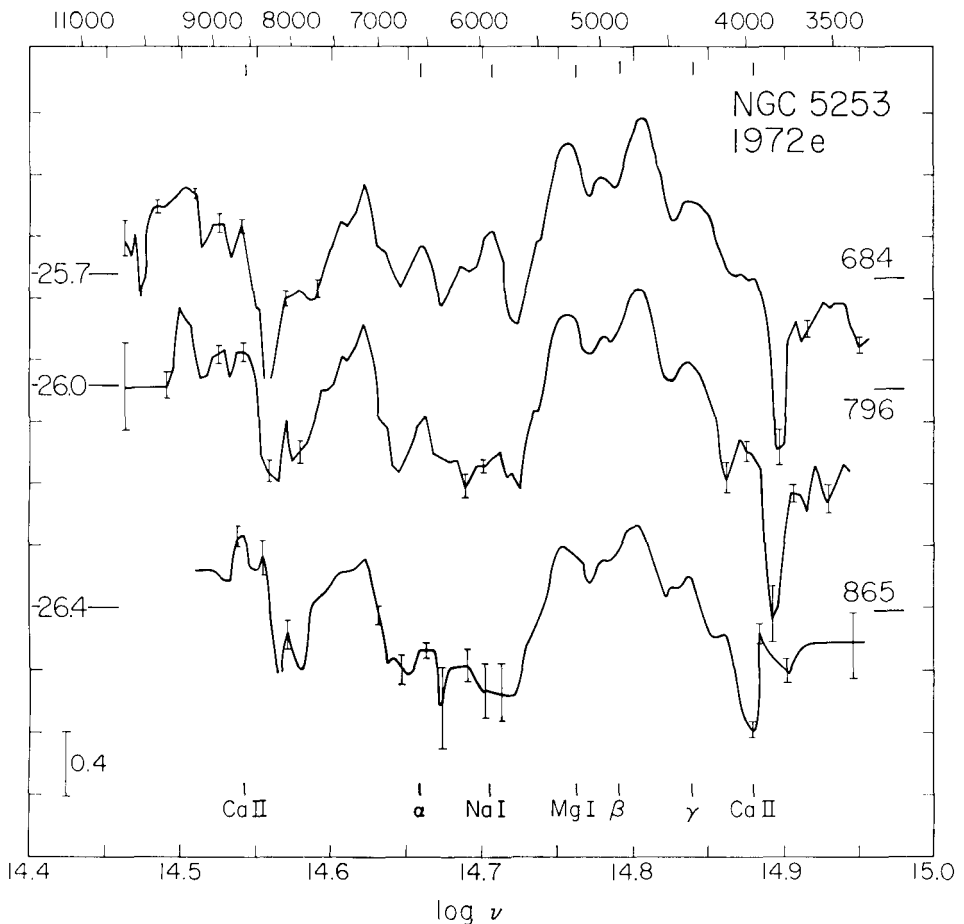

Fig. 5. Continuation of Figure 3. (By permission of the *Astrophysical Journal*.)

Real differences remain! Many other features, strong and weak, come and go in the confusing spectra of SN I's. The evidence for identifying these with well-known lines is far from compelling. The most puzzling feature is the emission at $\lambda 4600$ in the early phases of SN 1972e. Unlike other features, it drifts in wavelength to $\lambda 4700$ by JD 689, and has since been observed at $\lambda 4750$ on JD 865. Whether this can be explained in terms of Fe II is not clear.

In type II's, the Balmer series is clearly present, but in type I's, the question is more difficult. No traces of Balmer lines other than a possible weak Hα are seen
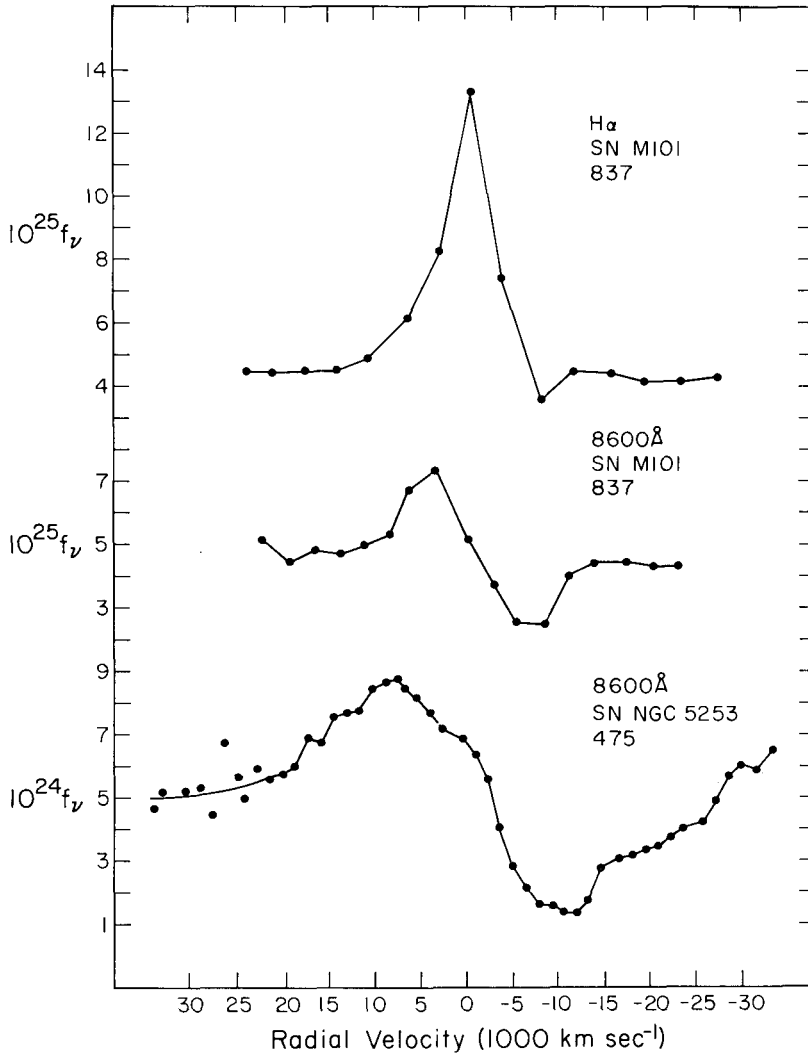

Fig. 6. Flux vs velocity shift (corrected to the rest wavelengths of each galaxy) for Hα and $\lambda 8600$ in the type II SN 1970g in M 101 on Julian Day 837, and for $\lambda 8600$ in the type I SN 1972e in NGC 5253 on Julian Day 475. (By permission of the *Astrophysical Journal*.)

in the first two weeks of the evolution of SN 1972e. However, on JD 460, a strong emission does appear in the expected position of Hα, and persists through JD 865. At about the same time, an emission feature appears in the position of Hγ. The spectra are too blended to determine whether Hβ is present. In Figure 2, the case for Balmer lines in type I is illustrated by comparison with type II. On the whole, the evidence in favor of Balmer lines seems good, but in a highly blended spectrum doubts must remain.

The conclusion seems inescapable that the main features which contribute to the spectra of SN II's are also prominent contributors to the spectra of SN I's. Generally line features are stronger and more numerous in SN I's. It is possible that a low hydrogen abundance in the envelopes of SN I's leads to more ions of common metals per free electron and hence stronger lines relative to the continuum.

3.4. SIMILARITIES AMONG SN I'S

Similarities among the light curves of SN I's are often cited as a striking property of these objects. (Zwicky, 1965). Our evidence from scans of four SN I's and comparison with SN 1937c is that the spectrum of any type I supernova can be identified with a particular epoch in SN 1972e. In this way, relative ages can be reliably-assigned.

3.5. LATE PHASES

Figure 5 presents the observations obtained 7, 10, and 14 months after the discovery of SN 1972e. Perhaps the most striking feature of this late evolution is how little change takes place in the spectrum. The principal features from $\lambda5500$ to $\lambda4000$ remain nearly constant in shape, while fading in brightness. The P Cygni feature at $\lambda5900$, attributed to Na I, does disappear by JD 865. Similarly, there is evidence that the Ca II absorptions at H and K and at $\lambda8600$ are disappearing in that scan. Further observations are planned for Winter 1973, when the supernova will be about 20 months old.

4. Concluding Remarks

Absolute energy distributions help establish the physical setting of the supernova explosion. The temperature is immediately available from the continuum shape, the bulk motions from the line shapes, and for type II, electron density from emission strengths. In this physical setting, plausible identifications are possible which account for all the strong features in SN II's, and some of the same identifications seem appropriate for SN I's.

Acknowledgements

References

Greenstein, J. L. and Minkowski, R.: 1973, *Astrophys. J.* **182**, 225.
Kirshner, R. P., Willner, S. P., Becklin, E. E., Neugebauer, G., and Oke, J. B.: 1973a, *Astrophys. J.
   Letters* **180**, L97.
Kirshner, R. P., Oke, J. B., Penston, M. V., and Searle, L.: 1973b, *Astrophys. J.* **185**, 303.
Oke, J. B.: 1969, *Publ. Astron. Soc. Pacific* **81**, 11.
Oke, J. B. and Schild, R.: 1970, *Astrophys. J.* **161**, 1015.
Patchett, B. and Branch, D.: 1972, *Monthly Notices Roy. Astron. Soc.* **158**, 375.
Searle, L.: 1971, *Astrophys. J.* **168**, 327.
Zwicky, F.: 1965, *Stars and Stellar Systems* **8**, 367.